Surface effect on forced vibration of DNS by viscoelastic layer under a moving load

S.A.H. Hosseini[*1], O. Rahmani[2], H. Hayati[3] and A. Jahanshir[1]

[1]*Buin Zahra Higher Education Center of Engineering and Technology, Imam Khomeini International University, Qazvin, Iran*
[2]*Smart Structures and New Advanced Materials Laboratory, Department of Mechanical Engineering, University of Zanjan, Zanjan, Iran*
[3]*Faculty of Engineering and Information Technology, University of Technology Sydney, PO Box 123, Broadway, Ultimo, NSW 2007, Australia*

Abstract. The surface effect for a forced vibration of a double-nanobeam-system (DNS) coupled by a viscoelastic layer under a moving constant load is studied in this paper. The viscoelastic layer that couples the nanobeams to each other, is modelled as spring-damper system. The Euler- Bernoulli theory and a simply supported boundary condition are considered for both nanobeams. By using the analytical solution, the dynamic displacement is obtained by considering the surface elasticity and residual tension effect on each nanobeams. Furthermore, the several significant parameters such as the velocity of the moving load, spring constant, damping coefficient and also the surface effect have been studied using some plots and examples. Finally, by observing the diagrams it was concluded that as the length of the beams reduces, the surface effect has a considerable effect on each of nanobeams especially at Nano scale, where it was not achieved by classic theories.

Keywords: double-nanobeam-system; forced vibration; surface effect; viscoelastic layer

1. Introduction

Recently nanomaterials have gained the attention of researcher communities in different fields such as physics, chemistry and engineering, due to their specific properties that are resulted by their nanoscale dimension (Murmu and Adhikari 2010). They are in the forms of different nanoscale structures such as nanoparticles, nanowires and nanotubes which exhibit promising mechanical, chemical, electrical, optical and electronic properties (Kim and Lieber 1999,; Liang, *et al.* 2015, Rakrak *et al.* 2016, Fernandes *et al.* 2017). Nanomaterials are considered as the basis of various nanoscale objects which are also named nanostructures (Fedorov *et al.* 2007, Choudhary and Kaur 2015). Nano-resonators, nano-actuators, nano-machins and nano-optomechanical systems are some of the commonest types of nanostructures (Eichenfield *et al.* 2009, El-Borgi *et al.* 2015, Reddy *et al.* 2016).

Based on the previous studies, it can be perceived that the material properties at the nano-scale

---

*Corresponding author, Ph.D., E-mail: Hosseini@bzte.ac.ir

are size dependent and subsequently the small length scale influence should be considered for an exact modelling of nano-structure (Pirmohammadi *et al*. 2014, Hosseini and Rahmani 2016, Ghadiri *et al*. 2018, Bastanfar *et al*. 2019, Alizadeh Hamidi *et al*. 2020, Hamidi *et al*. 2020; Hassannejad *et al*. 2020, Kunbar *et al*. 2020). To overcome this limitation, several modifications of the classical continuum mechanics have been presented to admit size effect in the nanostructures modelling. One broadly used size-dependent theory is the nonlocal elasticity theory (Pourseifi *et al*. 2015).

Various investigations are conducted to study nano sandwich structures. Liew *et al*. studied the vibration behaviour of multi-layered graphene sheets that were embedded in an elastic matrix using a continuum-based plate model. They derived an explicit formula to predict the natural frequencies and associated vibration modes of double-layered and triple-layered graphene sheets (Liew *et al*. 2006). Murmu *et al*. developed an analytical method to determine the natural frequencies of the nonlocal double beam, which are used in nano-optomechanical system and sensor applications. It was revealed that the small scale effect has a significant effect on the transverse vibration of double nanobeam system (Murmu and Adhikari 2010). In the other study, which was made by Murmu *et al*. the nonlocal vibration of double-nano-plate system, was considered. It was assumed that two nano-plates are bounded by an enclosing elastic medium. They established expression for bending vibration of double nano-plate system using the nonlocal elasticity and also introduced an analytical model to derive the natural frequencies of nonlocal double-nano-plate System (Murmu and Adhikari 2011). Pouresmaeeli *et al*. presented an analytical approach for free vibration analysis of all edges simply supported double orthotropic nano-plates. It was assumed that the two nano-plates are bonded by an internal elastic medium and surrounded by an external elastic foundation. They derived the governing equations according to the nonlocal theory (Pouresmaeeli *et al*. 2012). Murmu *et al*. analysed the vibration of coupled nanobeam system under initial compressive pre-stressed condition. Using the nonlocal theory expressions for bending-vibration of pre-stressed double nanobeam system is formulated. They also proposed an analytical method to obtain natural frequencies of the nonlocal double Nano-beam system. Radic *et al*. analysed buckling of double orthotropic nano-plates using the nonlocal elasticity theory. They assumed that two nano-plates are bounded by an internal elastic medium and are surrounded by external elastic foundation (Radić *et al*. 2014). Norouzzadeh *et al*. (2020) worked on flexural, axial, and shear wave propagation in nano FGMs by Eringen's integral model. Akgöz and Civalek (2017) surveyed the thermal and shear deformation effects on the responses of the non-homogeneous microbeam made of FGM. Akgöz and Civalek (2015) used the modified strain gradient theory along with the non-classical sinusoidal plate model to calculate the bending, buckling, and free vibration of the model. Demir and Civalek (2017) established an enhanced Eringen differential model to calculate the bending of the nano/micro Euler-Bernoulli beams for different loadings.

Yayli (2015) employed gradient theory considering the surface effect to obtain the stability of the beams with rotational and translational springs. Yayli (2016) carried out the axial vibration of nanorods by hardening the nonlocal approach by different boundary conditions. Yayli (2018) used nonlocal elasticity theory to obtain the torsional behavior of the carbon nanotubes embedded in elastic medium under the spring boundary conditions.

Alimirzaei *et al*. (2019) investigated the nonlinear static, buckling, and vibrational behaviors of the viscoelastic micro-composite beam having geometrical imperfection reinforced by different distributions of boron nitride, namely UD, FG-V, and FG-X based on the modified strain gradient theory and FEM. Darvishand and Zajkani (2019) carried out the plastic buckling behavior of the microbeams considering the small scale effect to evaluate the instability of the model, which is under boundary conditions, including simply supported, cantilever, and clamped-supported via

conventional mechanism-based strain gradient plasticity theory. Chaabane *et al*. (2019) studied the static and dynamic behaviors of the FG beams embedded in an elastic Winkler-Pasternak foundation based on the hyperbolic shear deformation theory. Hamed *et al*. (2019) worked on the bending behavior of the FG nanoscale beam model, having different types of porosity based on the Eringen's nonlocal elasticity theory. Gao *et al*. (2019) devoted their study to the free vibration of the FG circular nanotubes based on the nonlocal strain gradient theory considering the higher-order shear deformation beam model.

Aydogdu *et al*. (2018) worked on the longitudinal vibration of FG nanorods and nanobeams with variant nonlocal parameters based on the Ritz approach and stress gradient elasticity theory to assess the effect of the boundary condition and geometrical properties. Arda and Aydogdu (2017) conducted the axial vibration of carbon nanotubes attached with a damper based on the nonlocal stress gradient theory for two types of end conditions. Aydogdu and Arda (2016) employed the nonlocal classical elasticity theory to illustrate the forced axial vibration of nanorods. Hosseini *et al*. (2019) established different nonlocal theories via Eringen's model to investigate the free and forced axial vibrational behavior of the nanorod under clamped-clamped and clamped-free boundary conditions. Khosravi *et al*. (2020) employed two linear and harmonic loadings for zigzag SWCNT. The responses of the model were compared with other boron nitride and semiconducting nanotubes.

In the present paper, the surface effect for a forced vibration of a double-nanobeam-system coupled by a viscoelastic layer under a moving load is investigated. The viscoelastic layer is simulated as spring-damper system. The Euler-Bernoulli theory and a simple boundary condition are considered for both nanobeams. The analytical solution for the dynamic behaviour of nanobeams is obtained by considering the surface elasticity and residual tension effect.

2. Surface effect theory

The surface effects often play an important role in the mechanical and dynamic behaviour of nanostructures because of the increasing ratio between surface area and volume (Miller and Shenoy 2000, Sharma *et al*. 2003, Wang and Feng 2007). The surface elasticity is introduced by Gurtin *et al*. (1998) and since then has been utilised to explain various size-dependent scenarios at the nanoscale. The obtained results through this theory fit well with atomistic simulations and experimental measurements (Miller and Shenoy 2000, Dingreville *et al*. 2005). The energy which is associated by atoms in surface layers is different from the atoms in the bulk of material, which is called surface free energy. In most studies, this energy is neglected because it is introduced with a few layers of atoms near the surface, but in Nano size this energy cannot be ignored. In Nano scale this effect has dominant influence caused by its high ratio of surface to volume which the result is the higher elastic modulus and mechanical strength than classical studies.

The curvature of a bending beam can be approximated by $\partial^2 w / \partial x^2$. The Laplace–Young equation in Eq. (1) indicates that for a bending beam $\partial^2 w / \partial x^2$, the distributed transverse loading induced by the residual surface tension is

$$f = f_0 + H \frac{\partial^2 w}{\partial x^2} \tag{1}$$

Where the parameter H is a constant determined by the residual surface tension and the shape of cross section. For rectangle and circular cross sections, H is given, by
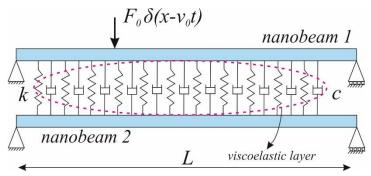
Fig. 1 Schematic of double nanobeam system under moving load

$$H = 2\tau^o D \tag{2}$$

Where τ° is the residual surface tension under unstrained condition and effective flexural rigidity, EI^*, for nanobeam is given by

$$EI^* = \frac{1}{4}\pi ER^4 + \pi E^s R^3 \tag{3}$$

E^s is the surface elastic modulus, which can be determined by atomistic simulations or experiments.

3. Governing equation for double nanobeam system

the double nanobeam system as illustrated in Fig. 1, the two nanobeams of the double beam system are referred to as nanobeam 1 and nanobeam 2. The two nanobeams are coupled by a viscoelastic medium. This medium is modeled as distributed spring-damped system. The primary nanobeam is assumed to be subjected to a concentrated transverse load $f(x,t)$. A secondary nanobeam is connected to the primary nanobeam by a viscoelastic material; where k is the spring constant and c is the damping coefficient. In general, two nanobeams may be different where the length, mass density per unit axial length and effective bending stiffness of the ith nanobeam are L_i, $\rho_i A_i$, $E_i I_i^*$ (i=1,2) respectively.

The transverse displacements of the primary and secondary nanobeams are $w_1(x,t)$ and $w_2(x,t)$, respectively.

The transverse vibration equation of the double nanobeam system are

$$E_1 I_1^* \frac{\partial^4 w_1}{\partial x^4} + k\left(w_1 - w_2\right) + c\left(\dot{w}_1 - \dot{w}_2\right) + \rho_1 A_1 \ddot{w}_1 - H_1 \frac{\partial^2 w_1}{\partial x^2} = f\left(x,t\right) \tag{4}$$

$$E_2 I_2^* \frac{\partial^4 w_2}{\partial x^4} + k\left(w_2 - w_1\right) + c\left(\dot{w}_2 - \dot{w}_1\right) + \rho_2 A_2 \ddot{w}_2 - H_2 \frac{\partial^2 w_2}{\partial x^2} = 0 \tag{5}$$

In this study, it is assumed that the two nanobeams have a same flexural rigidity (EI^*) and mass per unit length (ρA) and H.

$$E_1 I_1^* = E_2 I_2^* = EI^* \tag{6}$$

$$\rho_1 A_1 = \rho_2 A_2 = \rho A \tag{7}$$

$$H_1 = H_2 = H \tag{8}$$

Substituting the assumptions Eqs. (6)-(8) in Eq. (4) and Eq. (5)

$$EI^* \frac{\partial^4 w_1}{\partial x^4} + k\left(w_1 - w_2\right) + c\left(\dot{w}_1 - \dot{w}_2\right) + \rho A \ddot{w}_1 - H \frac{\partial^2 w_1}{\partial x^2} = f_0(x,t) \tag{9}$$

$$EI^* \frac{\partial^4 w_2}{\partial x^4} + k\left(w_2 - w_1\right) + c\left(\dot{w}_2 - \dot{w}_1\right) + \rho A \ddot{w}_2 - H \frac{\partial^2 w_2}{\partial x^2} = 0 \tag{10}$$

With a simple manipulation of variable, the transverse vibration equation of the double nanobeam system can be uncoupled and general analysis is used to determine the solution. In order to solve Eqs. (9) and (10), a change of variables by considering $w(x,t)$ is employed

$$w(x,t) = w_1(x,t) + w_2(x,t) \tag{11}$$

Thus

$$w_1(x,t) = w(x,t) - w_2(x,t) \tag{12}$$

Adding Eqs. (9) and (10) and using Eq. (12), would lead to

$$EI^* \frac{\partial^4 w}{\partial x^4} + \rho A \ddot{w} - H \frac{\partial^2 w}{\partial x^2} = f_0(x,t) \tag{13}$$

Substituting Eq. (12) into Eq. (10) leads to

$$EI^* \frac{\partial^4 w_2}{\partial x^4} + 2k w_2 + 2c \dot{w}_2 + \rho A \ddot{w}_2 - H \frac{\partial^2 w_2}{\partial x^2} = kw + c\dot{w} \tag{14}$$

The boundary conditions for nanobeams with two simply supported ends are given as

$$w_1(0,t) = w_2(0,t) = 0 \tag{15}$$

$$w_1(L,t) = w_2(L,t) = 0 \tag{16}$$

$$EI^* \frac{\partial^2 w_1(0,t)}{\partial x^2} = EI^* \frac{\partial^2 w_2(0,t)}{\partial x^2} = 0 \tag{17}$$

$$EI^* \frac{\partial^2 w_1(L,t)}{\partial x^2} = EI^* \frac{\partial^2 w_2(L,t)}{\partial x^2} = 0 \tag{18}$$

Note that Eq. (14) is identical to the governing partial differential equation of the forced vibration of an Euler-Bernouli nanobeam on a viscoelastic medium and Eq. (13) is that of uncoupled vibration equation.

4. Solution method

In this section, the Eqs. (13) and (14) are uncoupled. Firstly Eq. (13) should be solved for the relative displacement $w(x,t)$. Secondly, Eq. (14) should be solved for the displacement of the secondary nanobeam $w_2(x,t)$. At the end of this section, Eq. (12) leads to the displacement of the primary nanobeam $w_1(x,t)$.

4.1 Solution of undamped differential equation

Using the normal mode method, the solution of Eq. (13) is assumed to be a linear combination of the normal mode of the nanobeam as

$$w(x,t) = \sum_{n=1}^{\infty} W_n(x)\eta_n(t) \tag{19}$$

where $\eta_n(t)$ are the generalized coordinate and $W_n(x)$ are the normal mode of the simply supported nanobeam that are given by

$$W_n(x) = \sin(\frac{n\pi}{L}x) \tag{20}$$

Substituting Eq. (19) into Eq. (13) and multiplying by $W_j(x)$ and integrating from 0 to L, results in

$$\ddot{\eta}_n(t) + \omega_n^2\eta_n(t) = Q_n(t) \tag{21}$$

Where

$$\omega_n = \sqrt{\frac{EI^*\left(\frac{n\pi}{L}\right)^4 + H\left(\frac{n\pi}{L}\right)^2}{\rho A}} \tag{22}$$

In Eq. (13), term $f_0(x,t)$ is the external force which is function of x and t. For the case of constant moving point force, one can model the force using Dirac function

$$f_0(x,t) = F_0\delta(x - v_0 t) \tag{23}$$

where F_0 is the force magnitude acting on the nanobeam and v_0 is constant velocity of the moving load. In Eq. (21), $Q_n(t)$ is generalized force corresponding to the n th mode given by

$$Q_n(t) = \frac{1}{g_n}\int_0^L W_n(x)P_0\delta(x - v_0 t)\,dx = \frac{F_0}{g_n}\sin(\frac{n\pi}{L}v_0 t) \tag{24}$$

where

$$g_n = \int_0^L \rho A W_n^2(x)dx = \frac{\rho A L}{2} \tag{25}$$

In this study, the initial conditions are assumed to be zero

$$w_1(x,0) = w_2(x,0) = \dot{w}_1(x,0) = \dot{w}_2(x,0) = 0 \tag{26}$$

Substituting initial equation into Eq. (11) leads to

$$w(x,0) = \dot{w}(x,0) = 0 \tag{27}$$

Therefore, $\eta_n(t)$ can be expressed as

$$\eta_n(t) = \int_0^t Q_n(\tau)h(t-\tau)\,d\tau \tag{28}$$

with

$$h(t) = \frac{1}{\omega_n}\sin(\omega_n t) \tag{29}$$

Substituting Eq. (24) into Eq. (28) and considering Eq. (29), leads to

$$\eta_n(t) = \frac{2F_0}{\rho A L \omega_n}\int_0^t \sin[\omega_n(t-\tau)]\sin\left(\frac{n\pi v_0}{L}\tau\right)d\tau \tag{30}$$

Thus, the solution of Eq. (13) is given by (20) and (30)

$$w(x,t) = \frac{2F_0}{\rho A L}\sum_{n=1}^{\infty}\frac{\sin\left(\dfrac{n\pi}{L}x\right)}{\left(\dfrac{n\pi v_0}{L}\right)^2 - \omega_n^2}\left[\dfrac{\dfrac{n\pi}{L}v_0}{\omega_n}\sin(\omega_n t) - \sin(\frac{n\pi}{L}v_0 t)\right] \tag{31}$$

4.2 Solution of damping differential equation

Now $w_2(x,t)$ can be obtained from Eq. (14) by substituting Eq. (31) into Eq. (14) yields

$$EI^*\frac{\partial^4 w_2}{\partial x^4} + 2kw_2 + 2c\,\dot{w}_2 + \rho A\ddot{w}_2 - H\frac{\partial^2 w_2}{\partial x^2} = \frac{2F_0}{\rho A L}\sum_{n=1}^{\infty}\sin\left(\frac{n\pi}{L}x\right)P_n(t) \tag{32}$$

where

$$P_n(t) = \frac{k\left[\dfrac{\dfrac{n\pi}{L}v_0}{\omega_n}\sin(\omega_n t) - \sin\left(\dfrac{n\pi}{L}v_0 t\right)\right] + c\dfrac{n\pi}{L}v_0\left[\cos(\omega_n t) - \cos\left(\dfrac{n\pi}{L}v_0 t\right)\right]}{\left(\dfrac{n\pi}{L}v_0\right)^2 - \omega_n^2} \tag{33}$$

Once again, modal analysis is employed to solve Eq. (32)

$$w_2(x,t) = \sum_{n=1}^{\infty}W_{2n}(x)\eta_{2n}(t) \tag{34}$$

where W_{2n} is the n th normalized normal mode and $\eta_{2n}(t)$ is the n th generalized coordinate. W_{2n} is expressed as

$$W_{2n}(x) = \sin\left(\frac{n\pi}{L}x\right) \tag{35}$$

Similarly, substituting Eq. (34) into Eq. (32) and multiplying both side of the Eq. (32) by $W_{2i}(x)$, then integrating it from $x=0$ to L leads to

$$\ddot{\eta}_{2n}(t) + 2\omega_{2n}\xi_n\dot{\eta}_{2n} + \omega_{2n}^2\eta_{2n}(t) = Q_n^*(t) \tag{36}$$

where ω_{2n} and ξ_n denote the undamping natural frequency and damping ratio, respectively which are defined as

$$\xi_n = \frac{c}{\rho A \,\omega_{2n}} \quad , \quad \omega_{2n} = \sqrt{\frac{EI^*\left(\dfrac{n\pi}{L}\right)^4 + H\left(\dfrac{n\pi}{L}\right)^2 + 2k}{\rho A}} \tag{37}$$

Now, the generalized force related to the nth mode is obtained as

$$Q_n^*(t) = \frac{1}{g_n}\int_0^L W_{2n}(x)\frac{2F_0}{\rho A L}\sum_{n=1}^{\infty}\sin\left(\frac{n\pi}{L}x\right)P_n(t)dx \tag{38}$$

Substituting Eq. (25) into Eq. (38) and using orthogonality property

$$\int_0^L W_i(x)W_j(x)\,\mathrm{d}x = \delta_{ij} \tag{39}$$

where δ_{ij} is the Kronecker delta, leads to

$$Q_n^*(t) = \frac{2F_0}{\rho^2 A^2 L}P_n(t) \tag{40}$$

For zero initial condition, the generalized coordinate in the n th modes becomes as follows

$$\eta_{2n}(t) = \int_0^t \frac{1}{\omega_{2dn}}e^{-\xi_n\omega_{2n}(t-\tau)}\sin\left(\omega_{2n}(t-\tau)\right)Q_n^*(t-\tau)d\tau \tag{41}$$

where ω_{2dn} is the frequency of the damped vibration given by

$$\omega_{2dn} = \omega_{2n}\sqrt{1-\xi^2} \tag{42}$$

Substituting Eq. (37) into Eq. (38) and applying the integration leads to

$$\eta_{2n}(t) = \frac{2e^{-\xi\omega_{2n}t}F_0}{a_8}\left(\begin{array}{l} a_1\cos\left(\dfrac{n\pi v_0}{L}t\right)+a_2\sin\left(\dfrac{n\pi v_0}{L}t\right)+ \\ v_0 n\pi\left(a_3\cos(\omega_{2dn}t)+a_4\left(a_5\cos\left(\omega_n t\right)+a_6\sin\left(\omega_n t\right)\right)+a_7\sin(\omega_{2dn}t)\right)\end{array}\right) \tag{43}$$

where

$$a_1 = -v_0 n\pi L^2 e^{\xi\omega_{2n}t}\omega_n\omega_{2dn}\left(\begin{array}{l}\omega_n^4 + 2\omega_n^2\left(\xi^2\omega_{2n}^2-\omega_{2dn}^2\right) \\ +\left(\xi^2\omega_{2n}^2+\omega_{2dn}^2\right)^2\end{array}\right)\left(\begin{array}{l}v_0^2(n\pi)^2 c+ \\ L^2\left(\xi\omega_{2n}\left(2k-c\xi\omega_{2n}\right)-c\omega_{2dn}^2\right)\end{array}\right)$$

$$a_2 = e^{\xi\omega_{2n}t}L^3\omega_n\omega_{2dn}\left(\begin{array}{l}-v_0^2(n\pi)^2\left(k-2c\xi\omega_{2n}\right)+ \\ kL^2\left(\xi^2\omega_{2n}^2+\omega_{2dn}^2\right)\end{array}\right)\left(\begin{array}{l}\omega_n^4+2\omega_n^2\left(\xi^2\omega_{2n}^2-\omega_{2dn}^2\right) \\ +\left(\xi^2\omega_{2n}^2+\omega_{2dn}^2\right)^2\end{array}\right)$$

$$a_3 = \omega_n\omega_{2dn}\left(-v_0^2(n\pi)^2+L^2\omega_n^2\right)\left(\begin{array}{l}v_0^2(n\pi)^2\left(2k\xi\omega_{2n}+c\left(\omega_n^2-\left(\xi^2\omega_{2n}^2+\omega_{2dn}^2\right)\right)\right)+ \\ L^2\left(\begin{array}{l}2k\xi\omega_{2n}\left(\omega_n^2+2\xi^2\omega_{2n}^2-2\omega_{2dn}^2\right)- \\ c_v\left(\omega_n^2+3\xi^2\omega_{2n}^2-\omega_{2dn}^2\right)\left(\xi^2\omega_{2n}^2+\omega_{2dn}^2\right)\end{array}\right)\end{array}\right)$$

$$a_4 = e^{\xi\omega_{2n}t}\omega_{2dn}\left((v_0 n\pi)^4 + 2L^2(v_0 n\pi)^2\left(\xi^2\omega_{2n}{}^2 - \omega_{2dn}{}^2\right) + L^4\left(\xi^2\omega_{2n}{}^2 + \omega_{2dn}{}^2\right)^2\right)$$

$$a_5 = \omega_n\left(-2k\,\xi\omega_{2n} + c\left(-\omega_n^2 + \xi^2\omega_{2n}{}^2 + \omega_{2dn}{}^2\right)\right)$$

$$a_6 = \left(2c\,\omega_n{}^2\xi\omega_{2n} + k\left(-\omega_n^2 + \xi^2\omega_{2n}{}^2 + \omega_{2dn}{}^2\right)\right)$$

$$a_7 = \omega_n\left((v_0 n\pi)^2 - (L\omega_n)^2\right)\begin{pmatrix} -\left(k - c\xi\omega_{2n}\right)\left(\omega_n{}^2 + \xi^2\omega_{2n}{}^2\right)\left((v_0 n\pi)^2 + (L\omega_n)^2\right) + \\ \begin{pmatrix}(v_0 n\pi)^2\left(k + c\xi\omega_{2n}\right) \\ +L^2\left(k\,\omega_n{}^2 + c\,\omega_n{}^2\xi\omega_{2n} + 6k\,\xi^2\omega_{2n}{}^2 - 2c\xi^3\omega_{2n}{}^3\right)\end{pmatrix}\omega_{2dn}{}^2 \\ -L^2\omega_{2dn}{}^4\left(k + 3c\,\xi\omega_{2n}\right) \end{pmatrix} \tag{44}$$

$$a_8 = \left\{\begin{array}{l}\omega_n\omega_{2dn}\left(\rho A\right)^2\left((\omega_n - \omega_{2dn})^2 + (\xi\omega_{2n})^2\right)\left((\omega_n + \omega_{2dn})^2 + (\xi\omega_{2n})^2\right)\left(-(v_0 n\pi)^2 + (L\omega_n)^2\right) \\ \left((v_0 n\pi - L\omega_{2dn})^2 + (L\xi\omega_{2n})^2\right)\left((v_0 n\pi + L\omega_{2dn})^2 + (L\xi\omega_{2n})^2\right)\end{array}\right\}$$

After substituting the normalized normal mode Eq. (36) and generalized coordinate Eq. (43) into Eq. (35), the response of the secondary nanobeam is determined, finally the response of the primary nanobeam is achieved by Eq. (16).

5. Result and discussion

For the sake of validation, our results are compared to a condition with no moving load and damping and surface effect. Thus the free vibration of double and single beam with medium elastic layer is analysed and shown in Table 1 and the results are compared to Ref (Vu *et al*. 2000). One may clearly notice here that the Non-dimensional fundamental frequency parameters obtained in the present investigation are in excellent agreement to the results presented by an analytical solution and the results provided by Vu *et al*. (2000) for all cases that are used for comparison and validates the proposed method of solution. First of all, when the three parameters vanish (ξ=0, EI^*=0 and F_0=0) the classical isotropic beam theory is rendered.

The nondimesional parameter for result can be expressed as

$$\overline{W}_1 = \frac{w_1}{w_0}\quad,\quad \overline{W}_2 = \frac{w_2}{w_0}\quad,\kappa = \frac{kL^4}{EI}\quad,\quad \alpha = \frac{v_0}{v_{0cr}}\quad,\quad \bar{t} = \frac{v_0 t}{L}\quad,\quad U = \frac{E^s I^s}{EI}\quad,\quad \nu = \frac{HL^2}{EI}\tag{45}$$

Table 1 Dimensionless frequencies for single and double beam

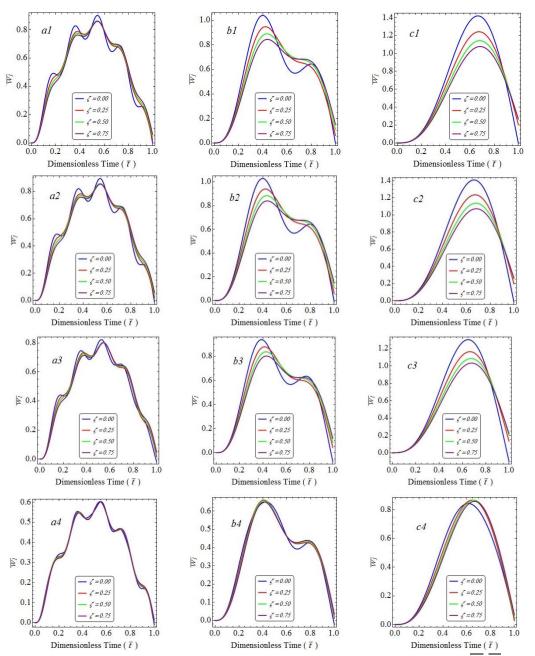| Mode number	Double beam				Single beam	
	K=10		K=800			
	(Vu *et al*. 2000)	Present	(Vu *et al*. 2000)	Present	(Vu *et al*. 2000)	Present
1	10.8355	10.835548	41.1996	41.199625	9.8696	9.8696044
3	88.9389	88.938947	97.4173	97.417331	88.8264	88.826440

Fig. 2 The variation of dimensionless dynamic response of the primary nanobeam ($\overline{W}_1\overline{W}_1$) versus dimensionless time ($\overline{t}\overline{t}$) for κ=0.1, 1, 10 and 100 and also α=0.1, 0.25 and 0.75

where $\overline{W}_1$ and $\overline{W}_2$ are the dimensionless displacement of the primary and secondary nanobeam in relation to w_0. w_0 is the maximum static deflection per F_0 loading for a beam with a simply support boundary condition at the middle of the beam and is equal to $w_0 = \dfrac{F_0 L^3}{48EI}$. κ and α are the

dimensionless stiffness and dimensionless velocity respectively which were dimensionalized in relation to v_{0cr}. It should be mentioned that v_{0cr} is a critical velocity and is equal to $v_{0cr} = \dfrac{\omega L}{\pi}$. $\overline{t}$ is the dimensionless time. U and v are dimensionless surface elasticity modulus and dimensionless residual surface tension, respectively. Before representing the results it should be noted that, displacement of each beam is considered at $x=L/2$. Also when $\overline{t} = 0$, the F_0 force is at the beginning of the left side of the nanobeam and when $\overline{t} = 1$, it is at the end of the right side of the nanobeam.

In this study the amount of U and η is considered to be 0.2 and 0.01 respectively, that indicates the influence of surface effect on $\overline{W}_1$ and $\overline{W}_2$. Fig. 2 shows the variation of $\overline{W}_1$ versus the dimensionless amount of time $(\overline{t})$ for different amounts of ξ. In Fig. 2(a1-a4) the variation of $\overline{W}_1$ is depicted for κ=0.1, 1, 10 and 100 respectively that in all the section α is equal to 0.1. Also in Fig. 2(b1-b4) and 2(c1-c4) $\overline{W}_1$ is depicted for α=0.25 and α=0.75 respectively. It can be seen from Fig. 2 that the $\overline{W}_1$ depends on the dimensionless amount of time $(\overline{t})$ that can increase or decrease its amount. Comparing all the sections of Fig. 2 with each others, it is clear that when κ increases from 0.1 to 100, the maximum dynamic deflection decreases and also when the moving load passes along the middle of nanobeam, the maximum dynamic deflection has its maximum amount.

It worth nothing to mention that in the absence of damping constant, for the negligible amount of κ, the coupling between nanobeams is not considerable which is so called "de-coupled". This condition is called "weak elasticity coupling". For high amounts of κ, there is considerable coupling between two nanobeams, which is called "rigid coupling".

According to Fig. 2 (b1-b4) when the moving load has passed along approximately 40% of the nanobeam, the maximum dynamic deflection of nanobeam has occurred. The maximum dynamic deflection of the primary nanobeam tends to occur when the moving load has passed along 60% of them beam which is shown in Fig. 2(c1-c4). As it is seen from all the sections of Fig. 2, increasing the damping coefficient (ξ) results in reduction of the maximum dynamic deflection which is considerable in Fig. 2 (c1) where the α is high and β is very low. In addition, the mentioned difference is considerably low in Fig. 2 (a4) because the system is in the rigid coupling mode.

Fig. 3 shows the variation of dynamic deflection of the secondary nanobeam $(\overline{W}_2)$ versus the dimensionless time $(\overline{t})$ for different damping coefficients. Fig. 3 (a1-a4) shows the variation of dynamic deflection for the dimensionless stiffness κ=0.1, 1, 10 and 100 respectively where in all of the sections, α is equal to 0.1. Figs. 3 (b1-b4) and 3 (c1-c4) show the dimensionless velocity for 0.25 and 0.5, respectively.

Based on Fig. 3 (b1-b4) the maximum dynamic deflection has occurred when the moving load passed along 40% of the nanobeam. Fig. 3 (c1-c4) shows that the maximum dynamic deflection tends to occur when the moving load passes along 65% of the nanobeam. By comparing the Fig. 3(a1), (1b) and (1c), it clear that in the weak elastic condition and when η=0, the dynamic deflection of secondary nanobeam is equal to zero. This is due to the transmission of dynamic deflection of the primary nanobeam to the secondary one caused by coupling. Comparing all the sections of Fig. 3, it can be concluded that as the ξ increases, the dynamic deflection increases where the maximum and the minimum of the difference between the mentioned parameters are shown in Fig. 3 (c1) and 3 (a4), respectively.

Fig. 4 shows the variation of the maximum dynamic deflection versus the dimensionless stiffness parameter from 0 to 1000. $W_{1,max}$, $W_{2,max}$ and W_{max} shows the variation of the maximum dynamic deflection of the primary nanobeam, the variation of the maximum dynamic deflection of the secondary nanobeam and the relative displacement of the primary and secondary nanobeam,
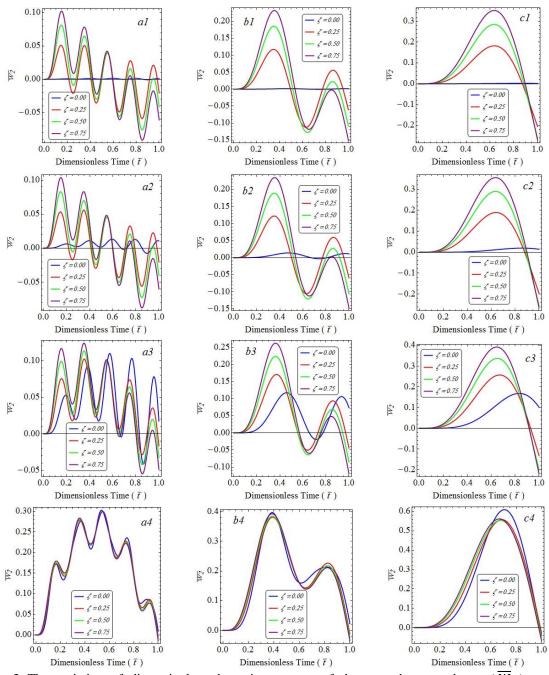
Fig. 3 The variation of dimensionless dynamic response of the secondary nanobeam ($\overline{W}_2$) versus dimensionless time ($\overline{t}$) for κ=0.1, 1, 10 and 100 and also α=0.1, 0.25 and 0.75

respectively. It can be seen that as the stiffness parameter increases the $W_{1,\max}$ and $W_{2,\max}$ decreases and increases respectively. As it can be seen from Fig. 4, increasing the κ in the rigid coupling condition caused in the convergence of $W_{1,\max}$ and $W_{2,\max}$ to each other and when κ=0, the difference
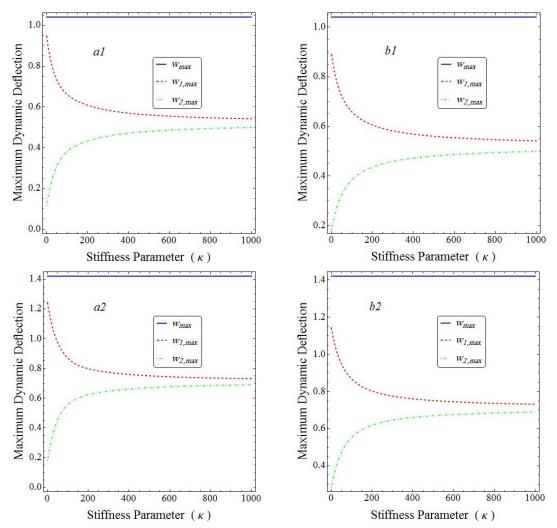
Fig. 4 The variation of the maximum dynamic deflection versus stiffness parameter. *a*1(*α*=0.25, *ξ*=0.25), *a*2(*α*=0.25, *ξ*=0.5), *b*1(*α*=0.5, *ξ*=0.25), *b*2(*α*=0.5, *ξ*=0.5)

between $W_{1,max}$ and $W_{2,max}$ is maximum. It worth nothing to mention that by comparing all the sections of Fig. 4 it can be concluded that the diagram of W_{max} is like a straight line that can be analysed in two different procedures. In the first procedure, the Eq. (31) is considered which shows that the relative displacement is independent of the stiffness and damping coefficient. Thus W_{max} is similar to a straight line. In the second procedure, by considering the Eq. (11), it is concluded that $W_{1,max}$ and $W_{2,max}$ are approximately symmetric in relation to each other

Fig. 5 shows the variation of maximum deflection versus the dimensionless velocity. Similar to Fig. 4, Fig. 5 has illustrated $W_{1,max}$, $W_{2,max}$ and W_{max} for *k*=1,10, 100 and1000. As it can be seen from this figure when *κ* increases, the maximum deflection increases and continues until 0.6 of dimensionless velocity. After that increasing the velocity of moving load causes in reduction of the maximum dynamic deflection. One other result that is derived from this figure, the diagram of $W_{1,max}$ is higher than the diagram of $W_{2,max}$ and as the *κ* increases these two diagrams come closer
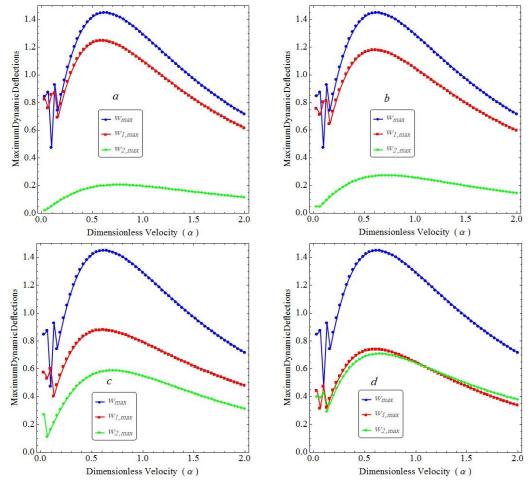
Fig. 5 The variation of the maximum dynamic deflection versus dimensionless velocity for *k*=1, 10, 100 and 1000

converges to each other. Fig. 5 presents the relation between the velocity of the moving load and the maximum dimensionless dynamic deflection at centre of the beam for various values of *k*. In Fig. 5, dimensionless velocity of the moving load ranges from $\alpha=0$ to $\alpha=2$ with 0.033 increments, and the maximum dimensionless dynamic deflections at the centre of the beams are plotted versus the corresponding velocities. In Fig. 5, it is clear that the velocity of the moving load has significant effect on the dynamic response of the beam. Note also that the maximum values of the displacements increase with increase in the velocity of the moving load until a certain value of the velocity of the moving load, and then decrease after this value of the velocity.

Fig. 6 illustrates the maximum dynamic deflection versus the surface elasticity modulus. it is seen from this figure, that as the surface elasticity modulus increases, the dynamic deflection decreases. Similar to prior figures the W_{max}, $W_{1,max}$ and $W_{2,max}$ are illustrated in this figure. According to the properties of introduced material and the dimensionless parameter u, it is concluded that, by decreasing the diameter from macro scale to nano one, the maximum dynamic deflection reduces, which shows the influence of the surface effect on dynamic displacement.
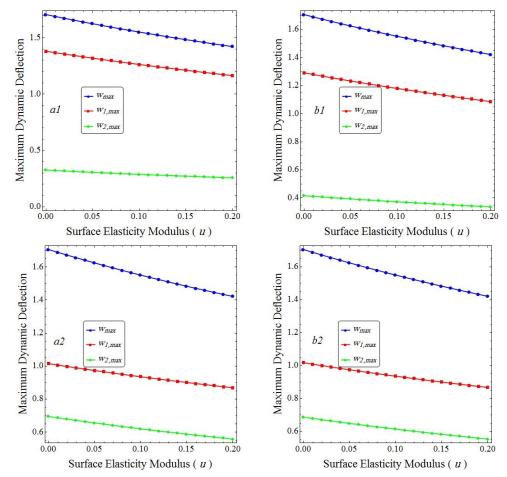
Fig. 6 The variation of dimensionless maximum dynamic deflection versus surface elasticity modulus. $a1(\beta=10, \xi=0.25)$, $a2(\beta=10, \xi=0.5)$, $b1(\beta=100, \xi=0.25)$, $b2(\beta=100, \xi=0.5)$

6. Conclusions

By considering the surface effect, this paper aims to analyse the forced vibration of a double nanobeam system that consists of a middle viscoelastic medium and is under a constant moving load. The viscoelastic medium was modelled as a spring-damper system. An analytical solution was presented for both nanobeams where the results were studied by dimensionalizing its parameters. Several diagrams for the dynamic displacement and the maximum dynamic deflection in terms of different parameters such as surface, the velocity of load movement, stiffness and damping parameter, were depicted. The results revealed that the amount of dynamic deflection for both nanobeams can increase or decrease in different times and perspecified parameters. It is also concluded that as the stiffness parameter increases, the maximum dynamic deflection of the primary and the secondary nanobeam decreases and increases respectively and finally converges to each other. Also increasing the dimensionless velocity results in the maximum amount of the maximum dynamic deflection in 0.6 of critical velocity. Finally, it is resulted that the classical theories cannot account for analysing the Nano scale structures because as the nanobeam diameter decreases from

macro scale to Nano scale the maximum dynamic deflection tends to reduce.

References

Akgöz, B. and Civalek, Ö. (2015), "A microstructure-dependent sinusoidal plate model based on the strain gradient elasticity theory", *Acta Mechanica*, **226**(7), 2277-2294. https://doi.org/10.1007/s00707-015-1308-4.

Akgöz, B. and Civalek, Ö. (2017), "Effects of thermal and shear deformation on vibration response of functionally graded thick composite microbeams", *Compos. Part B: Eng*., **129** 77-87. https://doi.org/10.1016/j.compositesb.2017.07.024.

Alimirzaei, S., Mohammadimehr, M. and Tounsi, A. (2019), "Nonlinear analysis of viscoelastic micro-composite beam with geometrical imperfection using FEM: MSGT electro-magneto-elastic bending, buckling and vibration solutions", *Struct. Eng. Mech*., **71**(5), 485-502. https://doi.org/10.12989/sem.2019.71.5.485.

Alizadeh Hamidi, B., Khosravi, F., Hosseini, S.A. and Hassannejad, R. (2020), "Free torsional vibration of triangle microwire based on modified couple stress theory", *J. Strain Anal. Eng. Des*., **55**(7-8), 237-245. https://doi.org/10.1177/0309324720922385.

Arda, M. and Aydogdu, M. (2017), "Longitudinal vibration of CNTs viscously damped in span", *Int. J. Eng. Appl. Sci*., **9**(2), 22-38. https://doi.org/10.24107/ijeas.305348.

Aydogdu, M. and Arda, M. (2016), "Forced vibration of nanorods using nonlocal elasticity", *Adv. Nano Res.*, **4**(4), 265. http://doi.org/10.12989/anr.2016.4.4.265.

Aydogdu, M., Arda, M. and Filiz, S. (2018), "Vibration of axially functionally graded nano rods and beams with a variable nonlocal parameter", *Adv. Nano Res.*, **6**(3), 257. http://doi.org/10.12989/anr.2018.6.3.257.

Bastanfar, M., Hosseini, S.A., Sourki, R. and Khosravi, F. (2019), "Flexoelectric and surface effects on a cracked piezoelectric nanobeam: Analytical resonant frequency response", *Arch. Mech. Eng*., **66**(4), 417-437. http://doi.org/10.24425/ame.2019.131355.

Chaabane, L.A., Bourada, F., Sekkal, M., Zerouati, S., Zaoui, F.Z., Tounsi, A., Derras, A., Bousahla, A.A. and Tounsi, A. (2019), "Analytical study of bending and free vibration responses of functionally graded beams resting on elastic foundation", *Struct. Eng. Mech*., **71**(2), 185-196. https://doi.org/10.12989/sem.2019.71.2.185.

Choudhary, N. and Kaur, D. (2015), "Vibration damping materials and their applications in nano/micro-electro-mechanical systems: a review", *J. Nanosci. Nanotechnol*., **15**(3), 1907-1924. https://doi.org/10.1166/jnn.2015.10324.

Darvishvand, A. and Zajkani, A. (2019), "Size-dependent plastic buckling behavior of micro-beam structures by using conventional mechanism-based strain gradient plasticity", *Struct. Eng. Mech*., **71**(3), 223-232. https://doi.org/10.12989/sem.2019.71.3.223.

Demir, Ç. and Civalek, Ö. (2017), "On the analysis of microbeams", *Int. J. Eng. Sci*., **121** 14-33. https://doi.org/10.1016/j.ijengsci.2017.08.016.

Dingreville, R., Qu, J. and Cherkaoui, M. (2005). "Surface free energy and its effect on the elastic behavior of nano-sized particles, wires and films", *J. Mech. Phys. Solid.*, **53**(8), 1827-1854. https://doi.org/10.1016/j.jmps.2005.02.012.

Eichenfield, M., Chan, J., Camacho, R.M., Vahala, K.J. and Painter, O. (2009), "Optomechanical crystals", *Nature*., **462**(7269), 78-82. https://doi.org/10.1038/nature08524.

El-Borgi, S., Fernandes, R. and Reddy, J.N. (2015), "Non-local free and forced vibrations of graded nanobeams resting on a non-linear elastic foundation", *Int. J. Nonlin. Mech*., **77** 348-363. https://doi.org/10.1016/j.ijnonlinmec.2015.09.013.

Fedorov, A.S., Novikov, P., Martinez, Y.S. and Churilov, G. (2007), "Influence of buffer gas and vibration temperature of carbon clusters on fullerene formation in a carbon plasma", *J. Nanosci. Nanotechnol*., **7**(4-5), 1315-1320. https://doi.org/10.1166/jnn.2007.309.

Fernandes, R., El-Borgi, S., Mousavi, S.M., Reddy, J.N. and Mechmoum, A. (2017), "Nonlinear size-dependent longitudinal vibration of carbon nanotubes embedded in an elastic medium", *Physica E: Low Dimens. Syst. Nanostruct.*, **88** 18-25. https://doi.org/10.1016/j.physe.2016.11.007.

Gao, Y., Xiao, W. and Zhu, H. (2019), "Nonlinear vibration of functionally graded nano-tubes using nonlocal strain gradient theory and a two-steps perturbation method", *Struct. Eng. Mech.*, **69** 205-219. http://doi.org/10.12989/sem.2019.69.2.205.

Ghadiri, M., Hosseini, S.A.H., Karami, M. and Namvar, M. (2018), "In-plane and out of plane free vibration of U-shaped AFM probes based on the nonlocal elasticity", *J. Solid Mech.*, **10**(2), 285-299.

Gurtin, M., Weissmüller, J. and Larche, F.J.P.M.A. (1998), "A general theory of curved deformable interfaces in solids at equilibrium", *Philos. Mag. A*, **78**(5), 1093-1109. https://doi.org/10.1080/01418619808239977.

Hamed, M.A., Sadoun, A.M. and Eltaher, M.A. (2019), "Effects of porosity models on static behavior of size dependent functionally graded beam", *Struct. Eng. Mech.*, **71**(1), 89-98. https://doi.org/10.12989/sem.2019.71.1.089.

Hamidi, B.A., Hosseini, S.A. and Hayati, H. (2020), "Forced torsional vibration of nanobeam via nonlocal strain gradient theory and surface energy effects under moving harmonic torque", *Wave. Rand. Complex Media*, 1-16. https://doi.org/10.1080/17455030.2020.1772523.

Hassannejad, R., Hosseini, S.A. and Alizadeh-Hamidi, B. (2020), "Influence of non-circular cross section shapes on torsional vibration of a micro-rod based on modified couple stress theory", *Acta Astronautica*, **178** 805-812. https://doi.org/10.1016/j.actaastro.2020.10.005.

Hosseini, S. and Rahmani, O. (2016), "Surface effects on buckling of double nanobeam system based on nonlocal Timoshenko model", *Int. J. Struct. Stab. Dyn.*, **16**(10), 1550077. https://doi.org/10.1142/S0219455415500777.

Hosseini, S.A., Khosravi, F. and Ghadiri, M. (2019), "Moving axial load on dynamic response of single-walled carbon nanotubes using classical, Rayleigh and Bishop rod models based on Eringen's theory", *J. Vib. Control.*, 1077546319890170. https://doi.org/10.1177/1077546319890170.

Khosravi, F., Hosseini, S.A. and Hayati, H. (2020), "Free and forced axial vibration of single walled carbon nanotube under linear and harmonic concentrated forces based on nonlocal theory", *Int. J. Modern Phys. B*, 2050067. https://doi.org/10.1142/S0217979220500678.

Kim, P. and Lieber, C.M. (1999), "Nanotube nanotweezers", *Sci.*, **286**(5447), 2148-2150. https://doi.org/10.1126/science.286.5447.214.

Kunbar, L.A.H., Alkadhimi, B.M., Radhi, H.S. and Faleh, N.M. (2020), "Flexoelectric effects on dynamic response characteristics of nonlocal piezoelectric material beam", *Adv. Mater. Res.*, **8**(4), 259. : https://doi.org/10.12989/amr.2019.8.4.259.

Liang, L.N., Ke, L.L., Wang, Y.S., Yang, J. and Kitipornchai, S. (2015), "Flexural vibration of an atomic force microscope cantilever based on modified couple stress theory", *Int. J. Struct. Stab. Dyn.*, **15**(07), 1540025. https://doi.org/10.1142/S0219455415400258.

Liew, K.M., He, X. and Kitipornchai, S. (2006), "Predicting nanovibration of multi-layered graphene sheets embedded in an elastic matrix", *Acta Materialia*, **54**(16), 4229-4236. https://doi.org/10.1016/j.actamat.2006.05.016.

Miller, R.E. and Shenoy, V.B.J.N. (2000), "Size-dependent elastic properties of nanosized structural elements", *Nanotechnol.*, **11**(3), 139.

Murmu, T. and Adhikari, S. (2010), "Nonlocal transverse vibration of double-nanobeam-systems", *J. Appl. Phys.*, **108**(8), 083514. https://doi.org/10.1063/1.3496627.

Murmu, T. and Adhikari, S. (2011), "Nonlocal vibration of bonded double-nanoplate-systems", *Compos. Part B: Eng.*, **42**(7), 1901-1911. https://doi.org/10.1016/j.compositesb.2011.06.009.

Norouzzadeh, A., Ansari, R. and Rouhi, H. (2020), "An analytical study on wave propagation in functionally graded nano-beams/tubes based on the integral formulation of nonlocal elasticity", *Wave. Rand. Complex Media*, **30**(3), 562-580. https://doi.org/10.1080/17455030.2018.1543979.

Özgür Yayli, M. (2016), "An efficient solution method for the longitudinal vibration of nanorods with arbitrary boundary conditions via a hardening nonlocal approach", *J. Vib. Control.*, **24**(11), 2230-2246. https://doi.org/10.1177/1077546316684042.

Pirmohammadi, A., Pourseifi, M., Rahmani, O. and Hoseini, S. (2014), "Modeling and active vibration suppression of a single-walled carbon nanotube subjected to a moving harmonic load based on a nonlocal elasticity theory", *Appl. Phys. A*, **117**(3), 1547-1555. https://doi.org/10.1007/s00339-014-8592-z.

Pouresmaeeli, S., Fazelzadeh, S. and Ghavanloo, E. (2012), "Exact solution for nonlocal vibration of double-orthotropic nanoplates embedded in elastic medium", *Compos. Part B: Eng.*, **43**(8), 3384-3390. https://doi.org/10.1016/j.compositesb.2012.01.046.

Pourseifi, M., Rahmani, O. and Hoseini, S.A.H. (2015), "Active vibration control of nanotube struct ures under a moving nanoparticle based on the nonlocal continuum theories", *Meccanica*, **50**(5), 1 351-1369. https://doi.org/10.1007/s11012-014-0096-6.

Radić, N., Jeremić, D., Trifković, S. and Milutinović, M. (2014), "Buckling analysis of double-orthotropic nanoplates embedded in Pasternak elastic medium using nonlocal elasticity theory", *Compos. Part B: Eng.*, **61** 162-171. https://doi.org/10.1016/j.compositesb.2014.01.042.

Rakrak, K., Zidour, M., Heireche, H., Bousahla, A.A. and Chemi, A. (2016), "Free vibration analysis of chiral double-walled carbon nanotube using non-local elasticity theory", *Adv. Nano Res.*, **4**(1), 31. http://doi.org/10.12989/anr.2016.4.1.031.

Reddy, J.N., Romanoff, J. and Loya, J.A. (2016), "Nonlinear finite element analysis of functionally graded circular plates with modified couple stress theory", *Eur. J. Mech.-A/Solid.*, **56** 92-104. https://doi.org/10.1016/j.euromechsol.2015.11.001.

Sharma, P., Ganti, S. and Bhate, N. (2003), "Effect of surfaces on the size-dependent elastic state of nano-inhomogeneities", *Appl. Phys. Lett.*, **82**(4), 535-537. https://doi.org/10.1063/1.1539929.

Vu, H., Ordonez, A. and Karnopp, B. (2000), "Vibration of a double-beam system", *J. Sound Vib.*, **229**(4), 807-822. https://doi.org/10.1006/jsvi.1999.2528.

Wang, G.F. and Feng, X.Q. (2007), "Effects of surface elasticity and residual surface tension on the natural frequency of microbeams", *Appl. Phys. Lett.*, **90**(23), 231904. https://doi.org/10.1063/1.2746950.

Yayli, M.Ö. (2018), "On the torsional vibrations of restrained nanotubes embedded in an elastic medium", *J. Brazil. Soc. Mech. Sci. Eng.*, **40**(9), 419. https://doi.org/10.1007/s40430-018-1346-7.

Yaylı, M.Ö. (2015), "Stability analysis of gradient elastic microbeams with arbitrary boundary conditions", *J. Mech. Sci. Technol.*, **29**(8), 3373-3380. https://doi.org/10.1007/s12206-015-0735-4.

CC